JOURNAL OF PROPULSION AND POWER
Vol. 15, No. 3, May–June 1999

Ion Beamlet Divergence Characteristics of Two-Grid Multiple-Hole Ion-Accelerator Systems

Yukio Hayakawa* and Shoji Kitamura*
National Aerospace Laboratory, Tokyo 182-8522, Japan

An experimental investigation was performed to determine the divergence characteristics (distortion factor, divergence angle, and divergence factor) of ion beamlets that were commonly formed using multiple-hole, ion-accelerator systems of ion thrusters. An isolated ion beamlet was observed three dimensionally using arrayed Faraday probes, and its divergence characteristics were determined as a function of geometrical grid parameters and grid voltages. Because xenon was used as a propellant and the grid voltages were chosen being conscious of a recent ion-thruster technology trend, the results can be used for designing ion thrusters by simply translating geometrical grid parameters. The results did not contradict those in previous studies that used argon and one- or two-dimensional beam diagnostics.

Nomenclature

d_a = accelerator-hole diameter, mm
d_s = screen-hole diameter, mm
d_{sp} = beamlet-separator-hole diameter, mm
F_d = distortion factor, s/S
f_D = divergence factor
J_b = beamlet current, A
J_i = ith probe current, A
L = axial distance between accelerator grid and probes, cm
l_{cc} = hole center-to-center distance, mm
l_e = effective acceleration length, mm
l_g = screen-to-accelerator-grid separation, mm
l_{sp} = accelerator-grid-to-separator separation, mm
NP/H = normalized perveance per hole, $A/V^{3/2}$
R = net-to-total voltage ratio, V_n/V_t
R_i = ith probe radial location measured from beamlet center, cm
S = beamlet-profile area, standard-circle area, mm^2
s = area outside of standard-circle beamlet profile, mm^2
t_a = accelerator-grid thickness, mm
t_s = screen-grid thickness, mm
V_a = accelerator-grid voltage, V
V_d = discharge voltage, V
V_n = net accelerating voltage, V
V_t = total accelerating voltage, $V_n - V_a$, V
θ_i = ith probe elevation measured from beamlet center, deg

Introduction

AN ion thruster is equipped with an ion-accelerator system that is composed of screen and accelerator grids, and a decelerator grid may be added to the system. Ions are extracted from discharge-chamber plasma and accelerated downstream applying voltage between these grids. Because the accelerated ions are not uniform in their final velocity vectors, they do not run in parallel. Many papers whose subjects were on the divergence characteristics of the ions were presented,[1,2] and it is known that the parameters that affect the divergence characteristics are grid-hole diameter, grid separation, grid thickness, and grid voltages. In most of the previous research, an ion beamlet was assumed to be axisymmetrical on one hand. On the other hand, the shapes of worn accelerator-grid holes[3,4] and three-dimensional ion-beamlet diagnostics[5] suggest that hexagonally symmetric distortion of ion-beamlet current density profiles occurs. (Because the distortions of each beamlet profile are in phase azimuthally, the composite profile of the complete ion beam is also distorted.[6,7]) This means that the ion-divergence characteristics obtained using the prevailing one- or two-dimensional beam diagnostics depend on the loci of probes (Fig. 1), that is to say, beam-divergence angle was not clearly defined in the previous studies. To estimate a beam-divergence angle correctly, three-dimensional beam diagnostics are required.

What the three-dimensional analysis exclusively contributes to ion-propulsion technology is the information on the behavior of an ion beamlet in relatively low-perveance cases. The knowledge given from this may not contribute to the innovative improvement of ion-extraction systems because the nominal operating point of a well-established ion-extraction system is located at relatively high perveance and the profile of an ion beam from it usually looks undistorted. In fact, the ion-beamlet profiles from circumstantial grid holes are expected to be distorted because the perveance is expected to be low there as a result of low plasma density near the discharge-chamber wall. The contribution from these beamlets to a whole ion beam is usually small and a distortion of the profile can be neglected. There are, however, two cases in which this knowledge plays an important role. First is the case with derated operation in which the perveance is apt to be low. The ion-beam profile tends to be distorted under the derated operation, and this knowledge may prevent diverged ions, that cannot be forecast otherwise, from impinging on the surface of a spacecraft. Derating will be limited to a given extent that is determined from the attitude and position of a thruster on the spacecraft using this knowledge. Second is the case with numerical ion-trajectory analysis. Many numerical codes for the three-dimensional analyses of ion-extraction systems have been developed.[8] Though such codes must be validated using experimental data, there are no three-dimensional experimental data available. Hence, two-dimensional data must be used. The results presented enhance three-dimensional code performance by introducing a factor to quantify the degree of ion-beamlet distortion. This will facilitate the comparison of numerical results with experimental data.

Adding grid-hole center-to-center distance to the preceding parameters, the manner in which variations in these parameters affected the ion-divergence characteristics was investigated using a single ion-beamlet generator and a three-dimensional beam-diagnostic system.

Presented as Paper 97-3195 at the AIAA/ASME/SAE/ASEE 33rd Joint Propulsion Conference, Seattle, WA, July 6–9, 1997; received Jan. 29, 1998; revision received Aug. 21, 1998; accepted for publication Sept. 16, 1998.

*Senior Research Officer, Space Technology Research Group, 7-44-1 Jindaijihigashi-machi Chofu. Member AIAA.

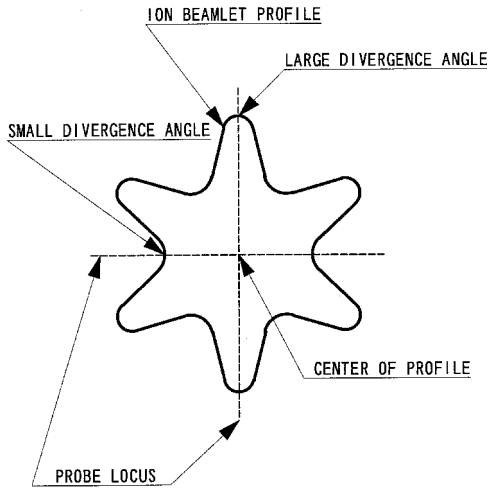

Fig. 1 Effect of probe locus on divergence angle.

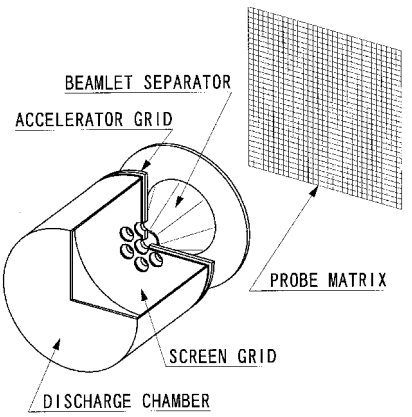

Fig. 2 Single ion-beamlet generator.

Apparatus

Single Ion-Beamlet Generator

A cutaway drawing of the single ion-beamlet generator used in this study is shown in Fig. 2. It consists of a discharge chamber from a 14-cm-diam ion thruster equipped with screen and accelerator grids that each have a centerline hole surrounded by six others. All of the screen-grid holes were electric-discharge machined so that the distortion of mechanical drilling would be avoided. The conical beamlet separator, which is shown downstream of the accelerator grid, has a 30-deg half-angle and it intercepted all beamlets, except the one at the thruster centerline. The separator was held at ground potential so that it played a role similar to that of a decelerator grid in a three-grid system. Both grids and the separator were made of stainless steel. Figure 3 defines symbols that represent the dimensions of the ion-accelerator system. The distance between the accelerator grid and separator was not precisely controlled. A standard geometry was defined to minimize the number of measurements. To investigate the effect of a geometrical variation, all dimensions except one were kept at the values shown next (in mm): $d_s = 4.0$, $d_a = 2.4$, $d_{sp} = 4.4$, $l_{cc} = 4.4$, $l_g = 2.0$, $l_{sp} = \sim 1$, $t_a = 1.0$, and $t_s = 0.6$.

Three-Dimensional Ion-Beam Diagnostic System

Thirty-two, 4-mm-diam-orificed Faraday probes (details in Fig. 4), arrayed vertically at 1-cm intervals on an X–Y stage, were used to measure ion-beamlet current density profiles. The probes were moved perpendicular to the beamlet axis in 1-cm increments, forming a 32×32 (1024 point) probe matrix to obtain ion-current densities at each element of the matrix (Fig. 2). Measurements were made 25 cm downstream of the accelerator grid. This distance was chosen through a previous work.[5] The probes and orifice plate were held at the ground potential. Four ammeters (three Keithley 486s and one 487) connected to a computer were used to measure and record the probe currents. The ammeters were operated in parallel and each was equipped with a mechanically relayed multiplexer that switched it through the eight probes. Collection of a complete data set required about $1\frac{1}{2}$ min. Probe currents were sensed by single measurements made through in-line analog and digital filters. An electrical schematic of the ion source and test facility is shown in Fig. 5. The ion-beamlet current was obtained summing the 1024 probe currents. Ambient-ion current was insignificant and secondary electron emission caused by one-kiloelectron-volt energized xenon–ion bombardment was expected to be insignificant.[9]

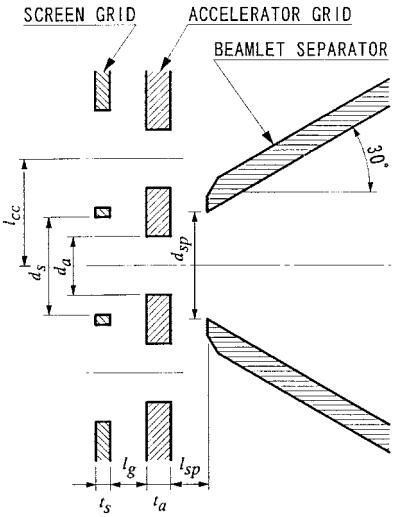

Fig. 3 Ion-accelerator system dimensions.

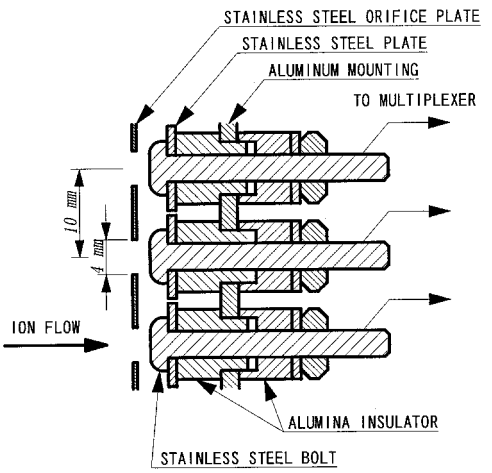

Fig. 4 Orificed Faraday probes.

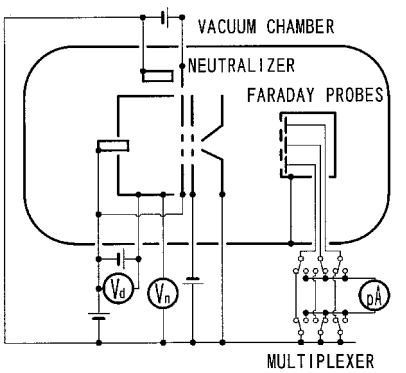

Fig. 5 Electric schematic of ion thruster and diagnostics.

Vacuum Facility

Both the ion-beamlet generator and diagnostics system were put in an 1.5-m-diam vacuum chamber pumped using two 55-cm-diam cryopumps. A typical base pressure reached after the experiment was 2.1×10^{-5} Pa.

Definitions

Normalized Perveance per Hole

There are three ways to define normalized perveance per hole.[10,11] In this study, it is defined as

$$NP/H = \left(J_b / V_t^{\frac{3}{2}} \right) (l_e / d_s)^2$$

where l_e is defined as

$$l_e = \left[(l_g + t_s)^2 + \left(d_s^2 / 4 \right) \right]^{\frac{1}{2}}$$

Distortion Factor

Distortions in the azimuthal uniformity of the ion beamlet are expressed using the concept of a distortion factor, which is determined following the procedure shown next (Fig. 6):

1) Determine the area of the beamlet-profile pattern ($=S$), defined as the equi-current-density contour that corresponds to 2.5% of the maximum ion-current density.

2) Draw a circle that is centered on the pattern at the maximum ion-current density location and has the same area as the pattern. This circle is named standard circle.

3) Determine the area of pattern that falls outside the standard circle and inside the outline of the pattern ($=s$).

4) Compute the distortion factor using $F_d = s/S$.

It is noteworthy that distortion factors never reached zero because data analyses were accomplished numerically and circles were represented as polygons.

Divergence Angle

Divergence angles are represented as half-angles of cones that enclose 95% of the beamlet current and is determined following procedure:

1) Add up 1024 probe currents, thereby determining the beamlet current as follows:

$$J_b = \sum_{i=1}^{1024} J_i$$

2) Select the largest probe current among 1024 probe currents using the partial-averaging method and designate the position of this probe as the beamlet center.

3) Arrange the 1024 probe currents in order of angle from the beamlet center to the radial location of the probe measured from the beamlet center. The angle associated with the ith probe current is defined as $\theta_i = \arctan(R_i / L)$, and L remained at 25 cm throughout this study.

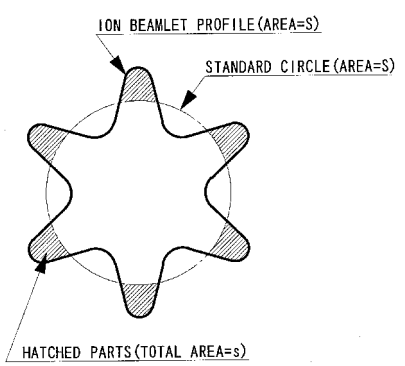

Fig. 6 Distortion factor.

4) Add up the probe currents sequentially until the sum reaches 95% of the beamlet current, thereby determining the angles on either side of the one that corresponds to 95% of the beamlet current.

5) Determine the divergence angle interpolating between these angles.

Divergence Factor

A divergent factor is determined as

$$f_D = \left(\sum_{i=1}^{1024} J_i \cos \theta_i \right) \Big/ J_b$$

Procedure

The beamlet generator was operated with a constant propellant flow rate of 25 mA (equivalent) through a hollow cathode and the neutralizer with a 40-mA (equivalent) flow rate. Some currents were always applied to both cathode heaters to maintain stable discharge with small flow rates, and a 0.2-A current was applied to the main cathode keeper. The beamlet current was varied by altering discharge current. Altering discharge current also varied the discharge voltage between 20 and 27 V through all experiments, though this was not intentional. The discharge current was increased or decreased between 0.1 and 0.6 A at 0.1 A intervals ($0.1 \rightarrow 0.2 \rightarrow \cdots \rightarrow 0.6 \rightarrow 0.5 \rightarrow \cdots \rightarrow 0.1$) to avoid radical conditional variation of the beamlet generator. When the beamlet current did not increase with the increase of discharge current, the upper limit of the discharge current was lowered. Net-accelerating voltage was altered between 1000 and 1200 V at 100-V intervals, whereas accelerator-grid voltage was altered between -100 and -300 V at 100-V intervals. Screen grid voltage was adjusted to keep the net-accelerating voltage constant while the discharge voltage was allowed to vary. The total accelerating voltage was obtained as the potential difference between the anode and accelerator grid ignoring the small sheath voltage. A standard case is defined as a combination of the standard geometry, 1100-V net accelerating voltage and -200-V accelerator-grid voltage.

The measurement was started after the beamlet-generator warming-up operation, which consisted of a >1-h discharge operation and >5 min of beamlet extraction. Vacuum chamber pressure was the highest at the beginning of the measurement and then gradually dropped. Lowest measured pressures were expected to be the closest to true pressures and were 4.3–4.6×10^{-4} Pa (not corrected for xenon). Highest pressures were about 3×10^{-5} Pa higher than the lowest pressures. The effect of the ion-beamlet-generator operational variation on the pressure was at most 1×10^{-5} Pa.

The probe currents were sensed at the 200-nA range. When the current exceeded the range, the range was switched to higher ones until it covered the current. The acquisition of a set of probe currents was not started until the stability of the discharge voltage was confirmed, except for a very gradual variation, every time the discharge current was altered.

Error Estimation

The accuracy of probe-current measurements depends on the accuracy of the ammeters and the magnitude of noise current that may originate from electrical noise and fluctuations in beamlet and background-plasma conditions. The magnitude of the noise current was always less than one-hundredth, and generally less than one-thousandth, of the largest probe current. The inaccuracy of the ammeters was insignificant compared with the noise magnitude. A 1% variation in the largest probe current has an insignificant effect on the distortion factor. Although beamlet profiles were not smooth in low-perveance cases, the distortion factors were generally reproducible and the variation of beamlet current determined by summing 1024 probe currents was less than 1% of the beam current. Measurements around the beamlet center most affect the results, because even a small variation in probe current may affect the determination of the beamlet-center location.

The spatial resolution of the measurement restricts both the resolutions of the distortion factor and divergence angle. Both resolutions generally decrease as divergence angle decreases if the spatial resolution is fixed. In this study, the resolution error in the divergence angle is theoretically less than 0.35 deg, when the divergence angle is larger than 10 deg. In practice, the variation in beamlet-center location must be also considered, and the errors caused by it are estimated to be less than 1.5% for the distortion factor and less than 0.5 deg for the divergence angle. The error introduced representing a smooth curve as segments in calculating the distortion factor is included in the preceding value.

The total errors are estimated to be less than 1.5% for the distortion factor and less than 0.85 deg for the divergence angle over all perveance values.

Experimental Results

To nondimensionize the geometrical grid parameters, they were divided by the screen-hole diameter (d_s) which remained at 4 mm throughout this study. Neither the net-accelerating nor accelerator-grid voltages were nondimensionized. All of the following figures showing the beamlet-divergence characteristics include data points at the standard case, although they are expressed in different ways. Because the divergence factor is similar to the inverse of the divergence angle, it is not commented on in the following text.

Effect of Grid Voltages

Figure 7 shows the effect of grid voltage variations on the beamlet divergence characteristics. The distortion is observed to decrease as perveance is increased, and because all of the data points fall along a common curve, it can be concluded that the distortion factor is independent of both the net accelerating and accelerator-grid voltages. This fact is common throughout this study. The data show that the general trend for divergence angle decreases with perveance to a minimum value and then rises slightly as perveance is increased further. All of the divergence-angle data points, except those for the case ($V_b = 1100$ V, $V_a = -100$ V), fall along a common curve. The divergence angle is weakly dependent on both the net accelerating and accelerator-grid voltages. This fact is also common throughout this study.

Effect of Screen Grid Thickness

Figure 8 shows the effect of screen-grid thickness variations on the beamlet divergence characteristics. The distortion factor is decreased as screen thickness is increased in the low-perveance region. When the thickness is 1.0 mm ($t_s/d_s = 0.25$), the distortion factor decreases with perveance to a minimum value, and then rises to a local maximum value as perveance is increased even more. The local maximum of the distortion factor and the minimum of the divergence angle are located closely in perveance. This is a general trend when the distortion factor is small, even in the low-perveance region. Although the real beamlet profile is circular, a smaller circle is expressed as a rougher circle in data processing because of the limitation of the probe spatial resolution. Three groups of divergence-angle data points fall along three independent curves, although they are very close to one another. Because the definition of normalized perveance per hole used in this study includes the screen grid thickness, the thickness has a great effect on the magnitude of perveance. If another definition is used, the three curves will fall apart. When geometrical grid parameters other than screen-grid thickness are changed, the altering definition causes few conceivable variations in the relative location of the curves. It is noted, however, that the horizontal axis must be rescaled when the definition is altered.

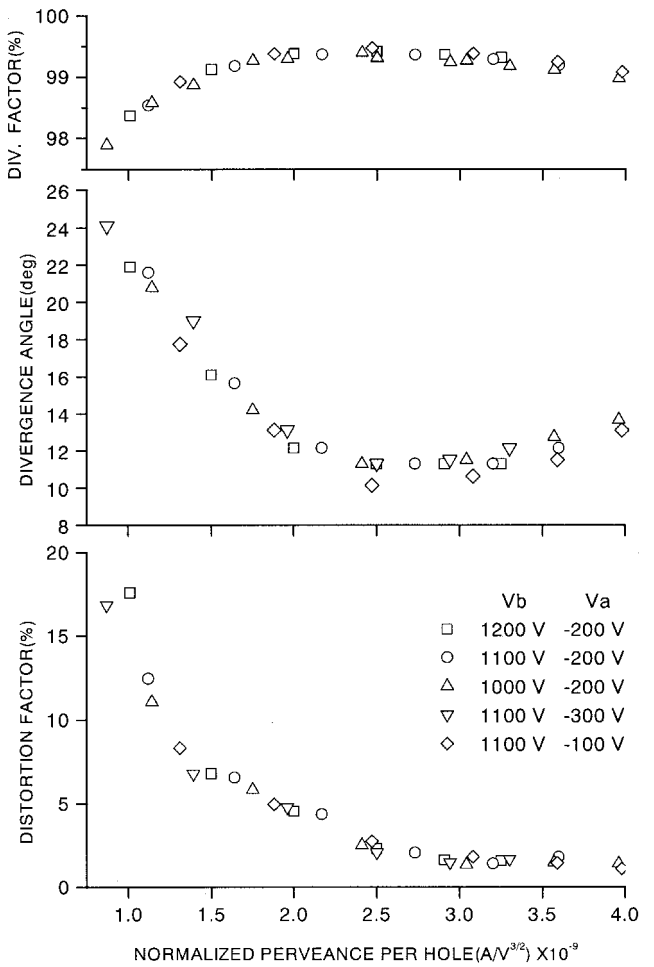

Fig. 7 Effect of net accelerating and accelerator-grid voltages on divergence characteristics.

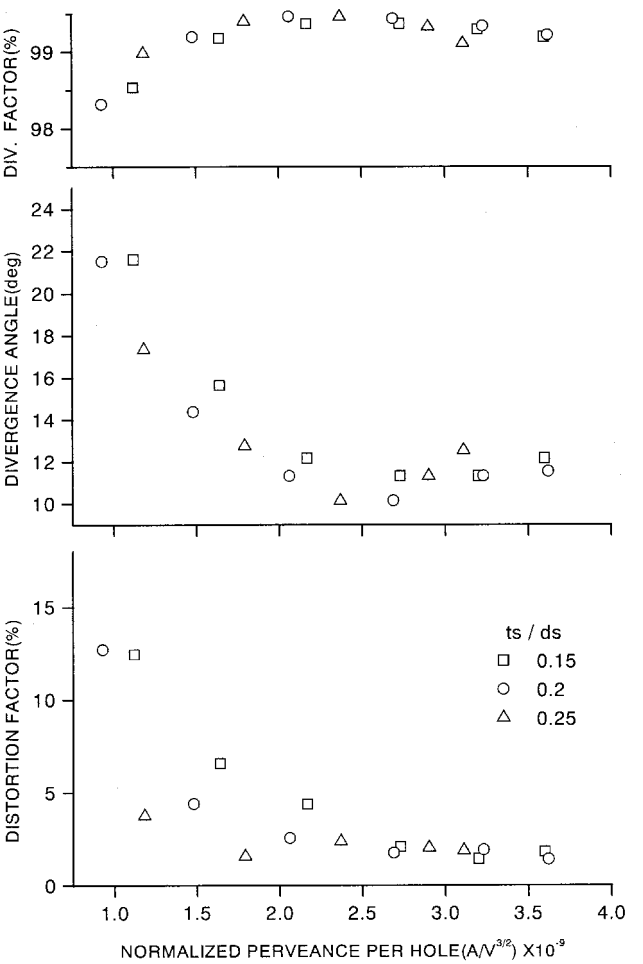

Fig. 8 Effect of screen-grid thickness on divergence characteristics.

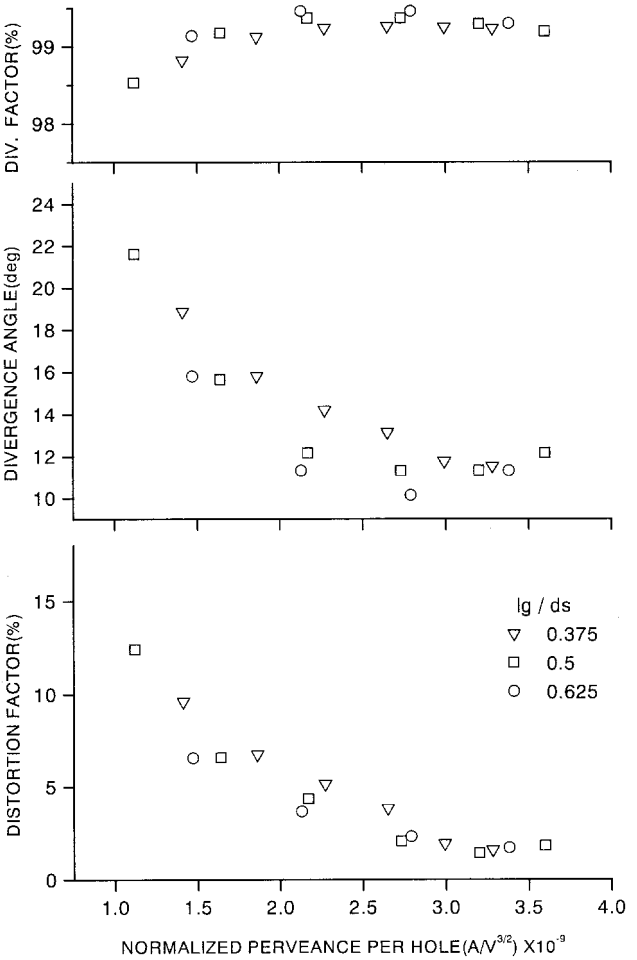

Fig. 9 Effect of grid separation on divergence characteristics.

Effect of Grid Separation

Figure 9 shows the effect of grid-separation variations on the beamlet-divergence characteristics. Both the distortion factor and divergence angle are decreased as grid separation is increased. Increasing the grid separation moves the minimum divergence angle to a lower value of normalized perveance per hole. It is noted, however, that the beamlet current is decreased as grid separation is increased.

Effect of Accelerator Grid Thickness and Hole Diameter

Figure 10 shows the effect of accelerator-grid thickness and accelerator-hole diameter variations on the beamlet-divergence characteristics. Both the distortion factor and divergence angle are independent of the accelerator-grid thickness and accelerator-hole diameter.

Effect of Hole Center-to-Center Distance

Figure 11 shows the effect of hole center-to-center distance variations on the beamlet-divergence characteristics. The distortion factor is decreased as distance is increased because the effect of the adjacent holes on the center beamlet is weakened. Each set of divergence-angle data points fall on an independent curve. The divergence angle is not linearly related to the distance.

Discussion

It is noteworthy that the distortion factor is independent of grid voltages, although it is likely that the variations of the voltages were too small to affect the divergence characteristics. The divergence-angle data obtained in this study can be compared with those in the previous studies.[1,11] In particular, the definition of normalized perveance per hole being in common with Ref. 11, both sets of data can be directly compared with each other. Table 1 shows principal differences in apparatus between this and the referenced studies. Two things must be remembered when the results of this work are compared with the previous ones. First is that the results of the previous works are with regard to an assembly of plural beamlets. When the number of beamlets is small, the influence of circumstantial beamlets that are not surrounded by six beamlets becomes significant and the profile of the beamlet assembly does not coincide with that of a beamlet that is surrounded by six beamlets. Second is that a probe rake was located on a line that included the center of an ion beam in the previous works. As was mentioned with Fig. 1, the relation between the line and grid-hole pattern must be clarified to define the divergence angle. Because of these two things, the divergence angle cannot be clearly defined when the profile is distorted in the previous works. In other words, this work clarifies the extent in which the results in the previous works are available, and the comparison of both results is possible when the perveance is sufficiently high. In Fig. 7, the variations in net-to-total accelerating voltage ratio are from 0.786 to 0.917. The divergence-angle variation caused by altering the net-to-total accelerating voltage ratio in this study looks slightly

Table 1 Differences in apparatus

Item	References[1,11]	This study
Propellant	Ar	Xe
Discharge chamber field	Divergent	Cusp
Cathode	Filament	Impregnated
Discharge voltage, V	40	20–27[a]
Pressure, $\times 10^{-4}$ Pa	73–113 (Ref. 1) 8.0–10.6 (Ref. 11)	1.7–1.8[b]

[a]Not controlled. [b]Corrected for Xe.

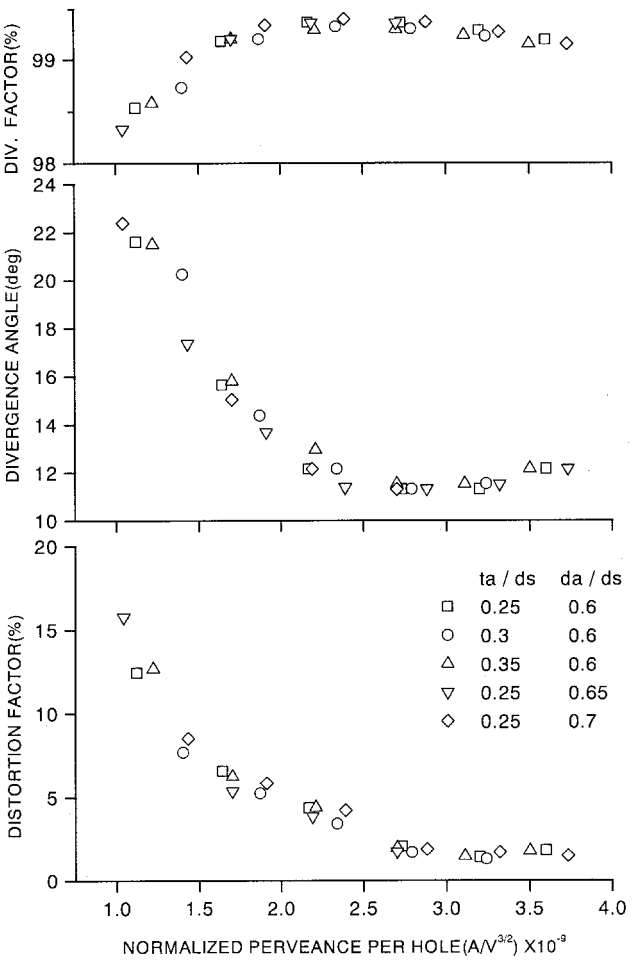

Fig. 10 Effect of accelerator-grid thickness and accelerator-hole diameter on divergence characteristics.

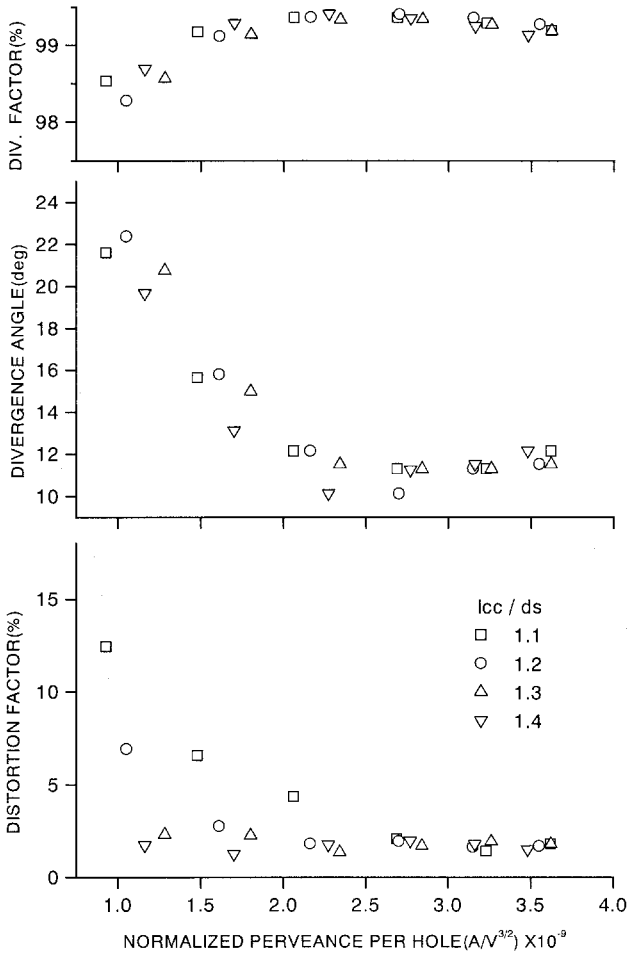

Fig. 11 Effect of hole center-to-center distance on divergence characteristics.

smaller than that in Ref. 1, whereas it shows a good agreement with that in Ref. 11. The divergence angles in this study are slightly smaller, within a few degrees, than those in the references, and this is probably a result of pressure differences.

The divergence-angle variation caused by altering screen-grid thickness or grid separation in this study looks similar to that in Ref. 1. Because both net-to-total accelerating voltage ratios do not coincide with each other, their magnitudes cannot be compared.

The divergence characteristics are independent of the accelerator-hole diameter and accelerator-grid thickness, and these trends are in common with Ref. 1. Their magnitudes cannot be compared. A smaller hole or a thicker grid is expected to decrease the upper limit of perveance.

Because recent xenon ion-thruster technology requires a discharge voltage between 28 and 30 V, it is preferable that the discharge voltage remains in this range. It was, however, impossible to raise the discharge voltage up to 28 V with the ion-beamlet generator used in this study. Reducing propellant flow rate might raise the discharge voltage, but it simultaneously caused unstable discharge operation. The variation in the discharge Ω voltage by altering cathode-heater current was quite small. As a result, controlling the discharge voltage was abandoned. The effect of discharge-voltage variations on the divergence characteristics is expected to be insignificant. Because of low discharge voltage, the effect of doubly-charged ions on the results is expected to be insignificant. Because the propellant utilization efficiency, which was calculated excluding the neutralizer flow rate, was at most, 9.2%, a significant amount of charge-exchanged ions were expected to be produced, and thus, probe currents may have been reduced. If the effect of charge-exchange collisions is assumed to be directionally uniform, the effect of the probe-current reduction on the divergence characteristics is canceled, although it may still affect beamlet current determination.

Conclusions

The following facts are confirmed concerning the effects of grid-voltage and geometrical grid-parameter variations on the beamlet-divergence characteristics:

1) Distortion factor is independent of grid voltages, accelerator-grid thickness, and accelerator-hole diameter, and is dependent on screen-grid thickness, grid separation, and hole center-to-center distance.

2) Divergence angle is independent of accelerator-grid thickness and accelerator-hole diameter, and is dependent on grid voltages (weakly), screen-grid thickness, grid separation, and hole center-to-center distance.

3) Divergence-angle data in this study did not contradict those of the previous studies, which used argon and one- or two-dimensional diagnostics, although they cannot be compared with one another in the low-perveance region.

References

[1] Aston, G., and Kaufman, H. R., "The Ion-Optics of a Two-Grid Electron Bombardment Thruster," AIAA Paper 76-1029, Nov. 1976.

[2] Kaufman, H. R., "Accelerator-System Solutions for Broad-Beam Ion Sources," *AIAA Journal*, Vol. 15, No. 7, 1977, pp. 1025–1034.

[3] Brophy, J. R., Pless, L. C., and Garner, C. E., "Ion Engine Endurance Testing at High Background Pressures," AIAA Paper 92-3205, July 1992.

[4] Hayakawa, Y., Miyazaki, K., and Kitamura, S., "Performance Test of a 14-cm Xenon Ion Thruster," AIAA Paper 92-3147, July 1992.

[5] Hayakawa, Y., Kitamura, S., and Miyazaki, K., "Beamlet Profiles from Multiple-Hole Ion-Extraction Systems," *Journal of Propulsion and Power*, Vol. 14, No. 4, 1998, pp. 568–574.

[6] Nakanishi, S., "Diagnostic Evaluations of a Beam-Shielded 8-cm Mercury Ion Thruster," NASA TM-78855, Jan. 1978.

[7] Groh, K. H., Fahrenbach, P., and Loeb, H. W., "Tests on the European Primary Radio-Frequency Engine ESA XX," AIAA Paper 94-3391, June 1994.

[8] Hayakawa, Y., "Three-Dimensional Numerical Model of Ion Optics System," *Journal of Propulsion and Power*, Vol. 8, No. 1, 1992, pp. 110–117.

[9] Carter, G., and Colligon, J. S., *Ion Bombardment of Solids*, Elsevier, New York, 1968.

[10] Kaufman, H. R., "Technology of Electron Bombardment Ion Thrusters," *Advances in Electronics and Physics*, Vol. 36, Academic, New York, 1974, pp. 265–373.

[11] Homa, J. M., "Ion Beamlet Steering for Two-Grid Electrostatic Thrusters," NASA CR-174671, July 1984.